Artifacts in femtosecond transient absorption spectroscopy

Article *in* Applied Physics B · January 2002

DOI: 10.1007/s003400100750

6 authors, including:

Maciej Lorenc
Université de Rennes 1
110 PUBLICATIONS **2,543** CITATIONS
SEE PROFILE

Marcin Ziolek
Adam Mickiewicz University
91 PUBLICATIONS **1,964** CITATIONS
SEE PROFILE

Ryszard Naskrecki
Adam Mickiewicz University
93 PUBLICATIONS **1,155** CITATIONS
SEE PROFILE

Jerzy Karolczak
Adam Mickiewicz University
142 PUBLICATIONS **2,306** CITATIONS
SEE PROFILE

Appl. Phys. B 74, 19–27 (2002)
DOI: 10.1007/s003400100750

Applied Physics B
Lasers and Optics

M. LORENC[1]
M. ZIOLEK[1]
R. NASKRECKI[1,✉]
J. KAROLCZAK[1]
J. KUBICKI[1]
A. MACIEJEWSKI[2]

Artifacts in femtosecond transient absorption spectroscopy

[1] Quantum Electronics Laboratory, Faculty of Physics, Adam Mickiewicz University, Umultowska 85, 61-614 Poznan, Poland
[2] Photochemistry Laboratory, Faculty of Chemistry, Adam Mickiewicz University, Grunwaldzka 6, 60-780 Poznan, Poland

Received: 29 May 2001/Final version: 15 October 2001
Published online: 29 November 2001 •

ABSTRACT The paper discusses three different artifacts related to two-photon absorption (TPA), stimulated Raman amplification (SRA) and cross-phase modulation (XPM), all intrinsic to transient absorption measurements with femtosecond time resolution. Certain properties of these signals are analysed and shown to superimpose onto measured transient absorption spectra. Ways of reducing the influence of the artifacts discussed are suggested. A simple correcting procedure based on the linear intensity dependence of the artifacts discussed is proposed.

PACS 07.60.-j; 42.62.Fi; 42.65.Re

1 Introduction

Transient absorption spectroscopy in ps and fs time domains is a powerful tool for the investigation of the dynamics of ultrafast photochemical and photophysical phenomena. It is a sensitive spectroscopic technique for studying the time evolution of excited states and the lifetimes of short-lived intermediates by measuring the time dependent transient absorption signal [1–3].

In a typical transient absorption experiment, two ultrashort laser pulses are incident on a sample in which they spatially overlap. An intense quasi-monochromatic laser pulse excites the sample, thus inducing photochemical or photophysical changes. These are monitored, as a function of time, by measuring relative absorption changes of a weaker broadband probe pulse. Temporal evolution of the created transient species – i.e. the response of the medium to the excitation – is obtained by measuring the absorption at different delay times between pump and probe pulses, varied continuously by using an optical delay line. The incoming and transmitted intensities of the probe pulse are detected simultaneously for a range of wavelengths using a multichannel detection system comprising a grating polychromator and PDA, or CCD, detector. The detection system reads out the time-integrated photoelectric signal as a function of time delay, thus no ultrafast electronics is needed. In this fashion a recording of transient absorption as a function of wavelength and time is obtained. Temporal resolution of such a system is determined by the laser pulse duration, the shortest delay between pump and probe pulses, the excitation geometry (i.e. the angle between pump and probe beams, their diameters and sample thickness) and the influence of the group velocity dispersion (GVD).

A number of possible artifacts might obscure fs transient absorption data, yet the most troublesome are those originating from the sample cells. The most significant causes of their appearance are:

– application of very short laser pulses (shorter than 100 fs), which results in extraordinary pump power density, usually 10–500 GW/cm^2, which easily encourages two-photon absorption (TPA) and stimulated Raman amplification (SRA);
– application of a spectrally very broad probe pulse, typically white light continuum in the 300–1100 nm range, which together with temporal chirp in the continuum and high pulse intensities inadvertently provides suitable conditions for efficient cross-phase modulation (XPM);
– a sensitive detection system, which allows observation of optical density changes on the order of 0.0005, means that unwanted signals of relatively low amplitude become comparable with weak transient signals.

The signals discussed have a common feature of being very short lasting upon excitation – their duration is comparable with the temporal width of the pump–probe cross-correlation function. Each of the signals is produced by the simultaneous action of two photons: one from the pump and the other from the probe, therefore their duration is directly related to the temporal response function. The spectral modifications within the probe upon pump-induced temporal changes of the refractive index lead to the appearance of XPM. Simultaneous absorption of a pump photon and a probe photon gives rise to TPA. The interchange of photons between pump and probe through a material's vibrational energy level gives rise to SRA. It should be noted that unwanted signals are likely to be generated both in the solutions studied (or pure solvents) as well as in commonly used fused silica windows of the sample cells.

2 Transient absorption experimental set-up

The apparatus used for the transient absorption measurements has been described in detail elsewhere [4, 5]

✉ Fax: +48-61/825-7758, E-mail: rysznas@amu.edu.pl

and only a brief description of the system will be given here. The fs laser system (Spectra Physics) comprises a titanium–sapphire oscillator (Tsunami) pumped by a second harmonic from a Nd:YVO_4 laser (Millenia), a regenerative optical amplifier on Ti:Al_2O_3 (Spitfire-F-1K) pumped by a second harmonic from a Nd:YLF laser (Merlin) and a generator for the second and third harmonics. The output of the laser system was set to work at 1 kHz repetition rate, providing pulses of duration between 80 and 120 fs, the energy of which reached 1 mJ. The output beam was tunable in the range 750 to 840 nm and had a Fourier-transform-limited bandwidth. The pump beam (usually IInd or IIIrd harmonic) was passed through a fixed optical path and was then focused inside the sample cell. The pump pulse waist was varied in the range 0.5–2 mm (FWHM). The probe beam was passed through an optical delay line consisting of two perpendicular flat mirrors mounted on a computer-controlled motorised translation stage and then converted to a white light continuum by focusing a fraction of the fundamental beam ($< 1\,\mu$J) in a rotating 1-mm-thick calcium fluoride plate. The probe's diameter was 2–5 times smaller than that of the pump.

To improve the signal to noise ratio, the measurements were performed in two-beam geometry (probe and reference), which allowed substantial elimination of the influence of the laser beam fluctuations and in consequence allowed the measurement of much smaller changes in optical density. In such a case, the measured signal was expressed by

$$S = \log \frac{I_{\mathrm{ref}}(\lambda)}{I_{\mathrm{probe}}(\lambda, \tau)} \tag{1}$$

where $I_{\mathrm{ref}}(\lambda)$ is the spectral intensity of a probing pulse travelling through an unexcited part of the sample (therefore time independent) and $I_{\mathrm{probe}}(\lambda, \tau)$ is the intensity of a probing pulse travelling through an excited part of the sample at time τ after excitation.

With this experimental set-up, the optical density of transient absorption and transient gain can be measured with the accuracy of 0.003 ΔOD from 370 nm to 700 nm. The temporal resolution was estimated from two-photon absorption measurements to be about 120 fs, within the available time window of 1.2 ns, whereas the spectral resolution in the whole visible range was approximately 1 nm.

The transient absorption measurements were carried out in a standard flowing sample cell with windows made from fused silica plates (0.5–1.25 mm thick) and an absorption layer of 0.2–2 mm thick. To avoid damage to the solid studied, the material was translated horizontally and vertically during measurements.

3 Unwanted signals

In spite of their unwanted contribution to the transient spectra, the unwanted signals can be also regarded as a source of important apparatus information. Investigation of these signals helps establish the system's essential parameters such as temporal resolution [6] or frequency chirp of the pump (SRA) and the probe pulses (TPA and XPM) [7].

3.1 *Two-photon absorption*

For low-intensity radiation ($< 10^{10}\,\mathrm{W/m^2}$) many simple molecular liquids and optical solids are transparent in the visible and near-UV spectral range. However, when high-power ultrashort laser pulses are applied, these media can absorb efficiently through a multiphoton absorption mechanism [8, 9].

On simultaneous absorption of n photons, the change of light intensity $I(x)$ along the optical path length x is given by

$$\frac{1}{I(x)}\frac{\partial I(x)}{\partial x} = -\gamma_n I^{n-1}(x) = (N_{\mathrm{g}} - N_{\mathrm{e}})\sigma_n \left(\frac{I(x)}{h\nu}\right)^{n-1} \tag{2}$$

where γ_n and σ_n are the n-photon absorption coefficient and n-photon absorption cross section, respectively, $h\nu$ is the energy of the incident photons and N_{g} and N_{e} are the population densities in the ground and excited states of the medium, respectively.

For sufficient power density of the light impinging on the sample in a pump–probe experiment, it is possible that two photons be absorbed simultaneously: one from the monochromatic pump and the other from the spectrally broad probe. The energy sum of these photons has to be greater than the energy corresponding to the long-wavelength limit of the material's absorption band. For laser pulses of 80 fs duration with a beam diameter of 0.7 mm (FWHM) and an energy per pulse between 0.1 and 40 μJ, the incident peak intensity varies between 10^{12} and $10^{15}\,\mathrm{W/m^2}$. It should be noted that at this intensity no visible signs of optical damage to fused silica or optical glass have been observed.

Absorption of light by a sample of thickness L will change the intensity of the passing light by following amount

$$\Delta I_{\mathrm{probe}} = \gamma \cdot I_{\mathrm{pump}} \cdot I_{\mathrm{probe}} \cdot L \ . \tag{3}$$

Making use of the expansion, $\ln(1+x) = x - 1/2x*x + 1/3x*x*x + \ldots$, the expression for transient absorption (1) was approximated by leaving only the first term. Introducing $I_{\mathrm{probe}} = I_{\mathrm{ref}} - \Delta I_{\mathrm{probe}}$, where $\Delta I_{\mathrm{probe}}$ denotes the amount of light absorbed by the sample, the approximated signal takes the form of

$$S_{\mathrm{aprox}} = 0.43 \cdot \frac{\Delta I_{\mathrm{probe}}}{I_{\mathrm{ref}}}. \tag{4}$$

The change in transient absorption signal is proportional to the amount of absorbed light and the error of this approximation is given by

$$\frac{S - S_{\mathrm{aprox}}}{S} = 1 - \frac{0.43}{S}(1 - 10^{-S}) \ . \tag{5}$$

This equals 2% when $S = 0.01$, 12% when $S = 0.1$ and 61% when $S = 1$. For typical TPA signals, when S is on the order of 0.01, this approximation seems totally justified. Therefore it is acceptable to assume that the TPA signal increases linearly with pump intensity. Such expectation has recently been proven correct in experiment [10].

The authors observed that TPA occurred in almost all the organic solvents investigated upon near-UV excitation (250–350 nm). When the excitation was tuned to the blue

(350–430 nm) visible, the TPA signal was only present in benzene and toluene. Amongst all the solids studied, the one which produced the strongest red-shifted TPA signal was the optical glass BK-7 (λ_{pump} =390 nm, $\lambda_{\text{probe}} \leq 550$ nm).

TPA kinetics, that is transient absorption change as a function of time for a given wavelength, measured in two BK7 plates of different thickness, 0.15 mm and 0.9 mm, are presented in Fig. 1. The TPA signal appears earlier at shorter wavelengths than at longer wavelengths, which is a consequence of the temporal distribution of the different Fourier components of the pulse – a feature called the chirp.

Temporal evolution of a TPA signal is a trace of the temporal chirp of spectral components of the white light continuum, which prompts making use of this signal to determine and then to correct the spectra for temporal chirp. Moreover its time dependence is a measure of the pump–probe cross correlation function. Thorough analysis showed a significant dependence of the signal's temporal width on the thickness and optical properties of the medium investigated. This dependence, resulting from velocity mismatch [11], causes temporal broadening of the TPA signal (Fig. 1).

Assuming a Gaussian shape for the pump–probe correlation function, that is the kinetics of the TPA signal, it is possible to show a strong modification of this function by the properties of the medium studied, which include medium length (sample thickness), wavelength difference between pump and probe pulses and dispersion of the refractive index [12]:

$$G_{\text{GVD}}(t) = G_0 \cdot \frac{\sqrt{\pi}}{4\sqrt{\ln 2}} \cdot \frac{\tau_{FWHM}}{\tau_{\text{GVD}}} \left[\text{erf}\left(\frac{2\sqrt{\ln 2}\, t}{\tau_{\text{FWHM}}} \right) - \text{erf}\left(\frac{2\sqrt{\ln 2} t}{\tau_{\text{FWHM}}} - \frac{2\sqrt{\ln 2}\tau_{\text{GVD}}}{\tau_{\text{FWHM}}} \right) \right] \quad (6)$$

where τ_{GVD} denotes the difference of passage time through the medium between the pump and probe pulses, G_0 is the amplitude of the unmodified pump–probe cross-correlation function (measured in a very thin sample) with FWHM equal to τ_{FWHM}. A broadening of 10% of the initial temporal width occurs when $\tau_{\text{GVD}}/\tau_{\text{FWHM}} > 0.6$. For values of the ratio above this number, the shape of the pump–probe cross-correlation function takes on a hat-like form. This significant change in shape is a consequence of pump–probe velocity mismatch, causing different time overlap of pump and probe pulses upon their propagation in the sample cell. Detailed explanation of this effect can be found in [12].

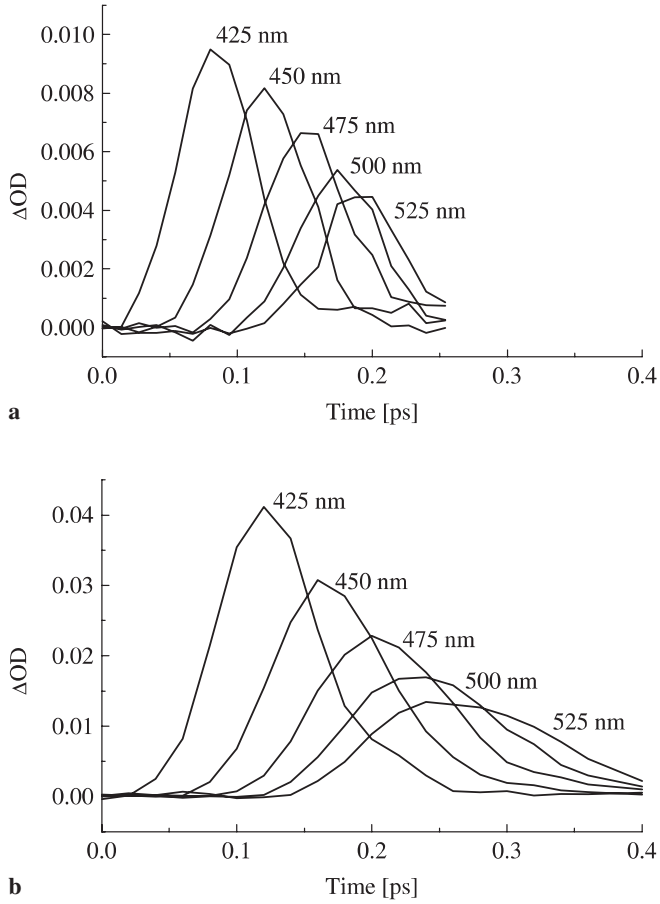

FIGURE 1 TPA signal measured in a plane-parallel BK7 optical glass plate of thickness 0.15 mm (**a**) and 0.9 mm (**b**). Excitation wavelength was 400 nm

3.2 *Stimulated Raman amplification*

A stimulated Raman amplification signal might occur during transient absorption measurements if the excitation wavelength is spectrally located close to the probe's wavelength. This condition being fulfilled gives rise to an apparent optical density change at a solvent-specific wavelength. The amplitude of this change is considerable but the whole effect vanishes after a time equal to the pump–probe cross-correlation. Raman amplification is a non-linear process coupling two laser beams, the pump and the probe, at Stokes frequencies, through material excitation. A rigorous mathematical treatment is elaborated elsewhere [7] and in this work we limit ourselves only to a qualitative discussion of the origin of SRA. SRA is generated if at least two photons, the laser's $h\nu_{\text{l}}$ and the Stokes $h\nu_{\text{s}}$, coincide in time and space inside the medium. Emission of a third photon can be stimulated provided that the energy of each of the incident photons differs by the amount corresponding to the molecular oscillation energy specific for each medium. In transient absorption systems $h\nu_{\text{l}}$ is carried with the pump pulse whereas $h\nu_s$ is provided by a suitable component of the probing white light continuum. The probe photons at wavelength λ_{SRA} seed the coupling between the molecular ground state and a virtual energy level through which the pump photons are scattered. Indeed, when the seeding photons were filtered out of the white light continuum, the SRA signal vanished completely. The importance of the white light continuum as the seed for generating the Raman lines by SRA has been reported earlier [13, 14].

SRA alone carries useful information on vibrational dynamics of scattering molecules, yet during transient absorption measurements it is an undesired effect. Nonetheless, its considerable amplitude, perfect reproducibility and appearance around time zero all make this signal convenient for establishing the temporal resolution of the system. In the study presented, the photons scattered into the seed (probe) pulse have lower energy than the pump pulse photons and match

Solvent/ bond stretched	SRA wavelength [nm]	Observed shift [cm^{-1}]
Acetonitrile/ –CH stretching	446	3089
Ethanol/ –CH stretching	443	2937
Benzene/ –CH stretching	445	3038
Hexane/ –CH stretching	442	2886
Water/ –OH stretching	453	3435

TABLE 1 Observed SRA lines for the solvents studied. The pump wavelength equals 392 nm; SRA given at the wavelength of maximal signal

the vibrational energy condition. The probe pulse then carries a negative ΔOD signal, as if emission took place. A reverse situation is also possible when the photons are scattered out of the seed pulse, which then carries positive ΔOD, as if absorption took place. In such a case the seed photons are more energetic than the pump photons. Spectrally, this translates into either a negative red-shifted or a positive blue-shifted signal with respect to the excitation wavelength. The authors investigated five different solvents in order to locate their SRA lines (Table 1). The signal amplitudes fell in the range between 0.02 and 0.04 of ΔOD and its duration, in the presence of pump photons at 392 nm and the white light continuum seeding photons, was found to be 120 fs, as for a Gaussian pulse shape.

The frequency of the amplified Stokes pulse might deviate from the value expected on the basis of spontaneous Raman data due to a non-linear phase modulation of the Stokes signal [15]. The combined effects of the frequency modulation and the Stokes generation cause a shift of SRA signal to higher frequencies (fewer cm^{-1} for the shift). Moreover, the SRA lines collected in Table 1 all appear red-shifted from the pump pulse and therefore they are called Stokes SRA. Normally these lines are accompanied by an anti-Stokes SRA signal which is blue-shifted from the pump and appears in the transient spectra with a reverse ΔOD sign (see above). In our experiments, the anti-Stokes lines were not observed due to the use of an optical filter placed in front of the detection system, to stop diffusing pump light.

The analysis of a SRA signal can provide important information on the pump pulse itself. Apart from laser pulse duration discussed earlier, the pump's temporal chirp can be determined. Time evolution of the SRA maximum towards shorter wavelengths is evidence of positive chirping within the pump pulse, see Fig. 2. When longer wavelengths are ahead of shorter ones within the pump they will interact with the probe earlier. The virtual energy level through which the process occurs is at first shifted slightly downwards and the SRA signal carried with the white light continuum will be detected at longer wavelengths. As the delay between pump and probe is increased, shorter wavelengths from the pump pulse begin to interact with the probe thus shifting the virtual level upwards and the SRA appears for shorter wavelengths of the continuum. It should be stressed that SRA intensity increases linearly with pump pulse intensity. This last observation was confirmed in a study of cyclohexane (Fig. 3a).

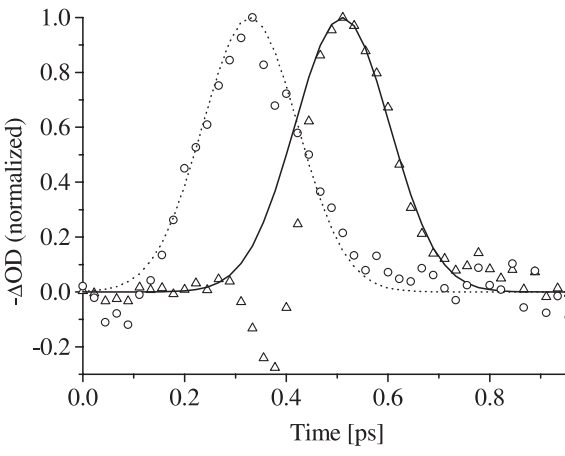

FIGURE 2 Normalized SRA signal measured in a 2 mm sample of acetonitrile, resulting from excitation at 400 nm, seeded with white light components at 445 nm and 450 nm, the wavelengths which correspond to spectral edges of the pump pulse. A 5-cm-long quartz rod was placed in the pump's path in order to increase the chirp. *Triangles*, experimental data at 445 nm; *circles*, experimental data at 450 nm; *dotted line*, numerical fit at 450 nm; *solid line*, data at 445 nm fitted within the limits where XPM perturbation (see Sect. 3.3) could be disregarded

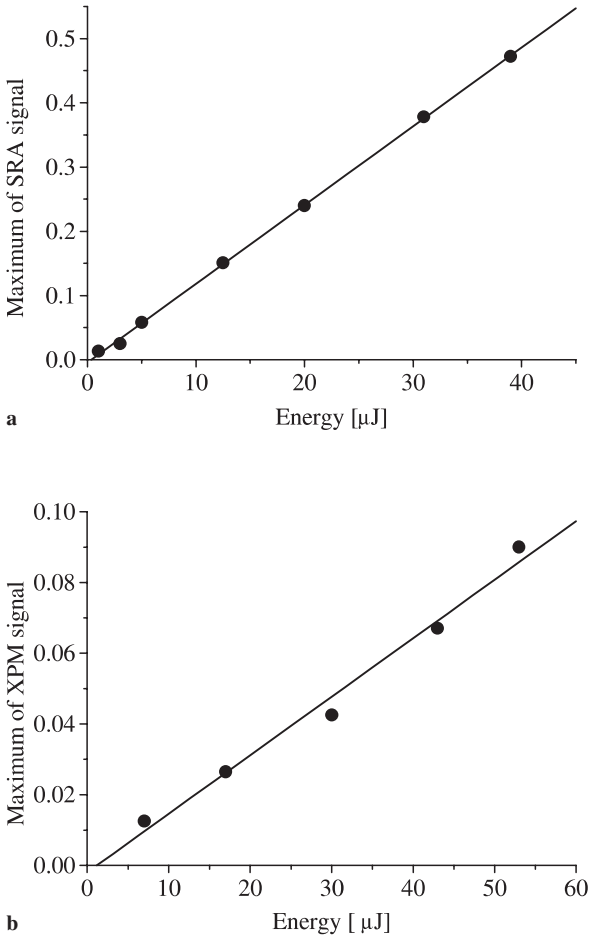

FIGURE 3 **a** The influence of pump pulse energy on SRA amplitude. 2-mm-thick sample with cyclohexane, pump pulse's diameter at FWHM equals 1.1 mm; **b** the influence of pump pulse energy on XPM signal. 2-mm-thick sample with acetonitrile, signal observed at probe's wavelength equal to 425 nm, pump pulse's diameter at FWHM equals 1.1 mm

Even though our observations only concern matter in a condensed phase, the effect has also been investigated, and taken advantage of, in the gas phase [16, 17].

3.3 *Cross-phase modulation*

Cross-phase modulation (XPM) generated in the liquid phase using the pump–probe technique has been reported by several authors [7, 11, 12, 18–20]. The XPM signal originates from empty cell windows (usually of fused silica) as well as from pure solvent contained in the cell. Cross-phase modulation is a non-linear process during which the intense pump pulse time dependently modulates the real part of the refractive index $n(t)$ of the optical medium

$$n(t) = n_0 + n_2 \mid A(t) \mid^2 \tag{7}$$

where $\mid A(t) \mid^2$ is the temporal envelope of the laser pulse.

When pump and probe pulses overlap in space and time, this modulation is experienced by the spectrally broad probe pulse and as a result the spectral distribution of the probe pulse is modified. This too gives rise to an unwanted signal around the time-zero point. It should be noted that the mechanism involves no net energy transfer into or away from the probe and occurs when the medium is completely transparent.

Below, the authors describe a simplified model of the XPM process, which conveys the nature of the process to a satisfactory extent.

In pump–supercontinuum-probe type experiments, the pump pulse has a much greater intensity than the probe pulse, which implies that any modification of the probe's frequencies is imposed by the pump pulse and not due to self phase modulation (SPM). Assuming linearly polarised light, homogenous spatial distribution of the pulses and a slowly-varying-envelope approximation, the following expression can be obtained for the probe's frequency shift [11, 18]

$$\Delta\omega(t) = -2\frac{n_2\omega_0 L}{c}\frac{\partial}{\partial t} \mid A(t) \mid^2, \tag{8}$$

where L stands for the sample (medium) thickness and ω_0 is the central frequency of the probe pulse.

This formula resembles the one for SPM, yet here the frequency modulation is greater by a factor of two. Within the time interval of the pump–probe interaction, the probe continuum can be assumed to have linear temporal chirp. Then, the frequency distribution within the reference and the probe pulses are described in the following way

$$\omega_{\mathrm{ref}}(t) = \omega_0 + \beta t \tag{9a}$$

$$\omega_{\mathrm{probe}}(t) = \omega_0 + \beta t + \Delta\omega(t) \tag{9b}$$

where β determines the linear chirp of the continuum components. From (9a,b) it follows that small β implies larger chirp, as fewer frequencies fall into any given time interval and thus are better temporally separated. Conversely, large β gives a smaller chirp of the probe.

Taking into account the frequency distribution (8) and assuming for the pump pulse a Gaussian shape with zero chirp

$$A(t) = A_0\,\mathrm{e}^{-t^2/\tau^2}\ , \tag{10}$$

the following expression is derived

$$\omega_{\mathrm{probe}}(t) = \omega_0 + \beta t + \frac{\alpha\omega_0}{\tau^2} t\,\mathrm{e}^{-2t^2/\tau^2}\ , \tag{11}$$

where α is given by

$$\alpha = \frac{8n_2 L A_0^2}{c}\ . \tag{12}$$

Figure 4 depicts the frequency modulation as a function of time. A set of parameters used in numerical simulations, expressed in arbitrary units, was chosen such that the frequency modulation effect is very clear.

Let us assume that for a given time delay between pump and probe pulses, within the range of frequencies interacting with the pump pulse, the light intensity is constant. Due to the interaction, the frequencies carried within the probe pulse are shuffled in such a way that those interacting with pump pulse's maximum are pushed outwards, resulting in intensity weakening of the central part of the probe pulse, where the density of frequency modes is decreased, and amplification of the probe pulse wings, where the density of frequency modes is increased. As can be seen from Fig. 4a, at $t = -50$ the slope of the perturbed distribution of probe pulse frequencies (dotted) becomes greater than the slope of the unperturbed distribution of probe pulse frequencies (solid). For the signal this translates into a reversal of ΔOD sign from negative to positive (Fig. 4b). The opposite happens at $t = 50$.

Despite its solely qualitative character, Fig. 4 still provides interesting information. The diagram of frequency depen-

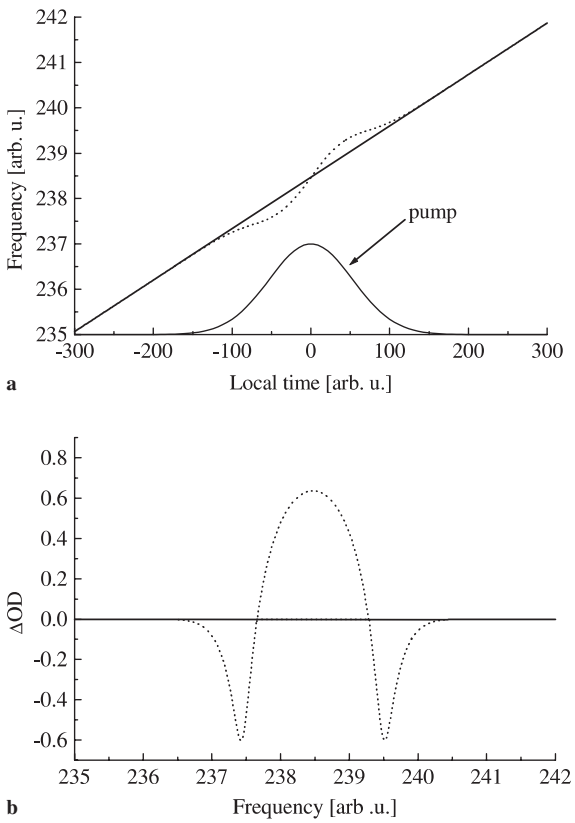

FIGURE 4 Simulation of the XPM signal; *dotted*, perturbed distribution of probe's frequencies due to XPM; *solid line*, unperturbed distribution of probe's frequencies (**a**); resulting modification of ΔOD signal's shape (**b**)

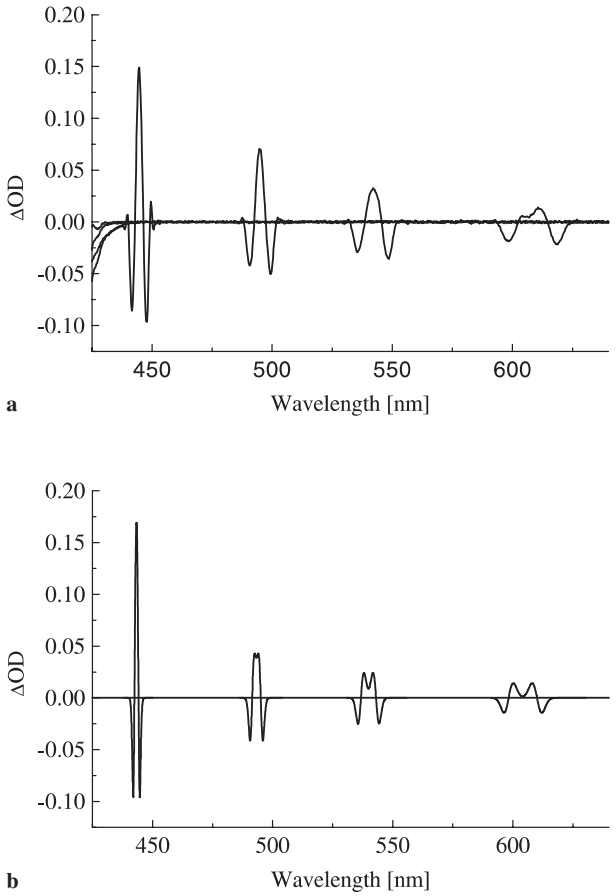

FIGURE 5 **a** Four selected XPM spectra as observed at different time delays corresponding to following probe wavelengths: 445 nm, 495 nm, 545 nm and 610 nm. Spectra measured in 2.5-mm-thick sample with acetonitrile; **b** Simulation of optical path was modified by introducing 100 mm of MeOH in order to significantly increase probe's temporal chirp. Simulation of this signal with (14) assuming conditions close to those in the experiment: FWHM = 120 fs, power density of 120 GW/cm^2, $n_2 = 10^{-16}$ cm^2/W

dence on time always features a dip appearing before a peak. Their depth and height depend on the α coefficient, time duration of the pump pulse and the frequency ω_0.

The magnitude of the perturbation of the linear chirp with respect to the linear chirp coefficient (β) determines the intensity of the induced XPM signal, which means greater signal for higher frequencies and greater probe chirp. The greater is the chirp, the larger is the time separation between neighbouring frequencies of the probe, so that fewer frequencies fall into the interval of interaction with the pump. This translates into a smaller slope in Fig. 4 (top) and therefore increased XPM signal.

In the opposite case, when chirp is negative, the slope changes sign and XPM behaves likewise (dipped middle and peaked wings).

By treating the problem quantitatively, the following formula can be derived for the signal in time domain (see Appendix for details)

$$S(t) = 2\log\left(1 + \frac{\alpha\omega_0}{\beta\tau^2\tau_{\mathrm{GVD}}}\left(t\,\mathrm{e}^{-2t^2/\tau^2} - (t-\tau_{\mathrm{GVD}})\,\mathrm{e}^{-2(t-\tau_{\mathrm{GVD}})^2/\tau^2}\right)\right). \tag{13}$$

Now, converting time to frequency (assuming that frequency modulation due to XPM is small compared to the modulation imposed by chirp, $\omega = \omega_0 + \beta t$) and then to wavelength, i.e. $t \to (\omega - \omega_0)/\beta$ and $\omega \to 2\pi c/\lambda$, leads to the following formula for the signal in the wavelength domain

$$S(\lambda) = 2\log\left(1 + \frac{\alpha\lambda_0}{\tau^2\tau_{\mathrm{GVD}}}\left(\frac{\mathrm{d}\tau_{\mathrm{disp}}}{\mathrm{d}\lambda}\right)(X - Y)\right) \tag{14}$$

where

$$X = \lambda_0^2\left(\frac{\mathrm{d}\tau_{\mathrm{disp}}}{\mathrm{d}\lambda}\right)\left(\frac{1}{\lambda} - \frac{1}{\lambda_0}\right)\mathrm{e}^{-2\left(\lambda_0^2\left(\frac{\mathrm{d}\tau_{\mathrm{disp}}}{\mathrm{d}\lambda}\right)\left(\frac{1}{\lambda}-\frac{1}{\lambda_0}\right)\right)^2 \Big/ \tau^2}$$

$$Y = \left(\lambda_0^2\left(\frac{\mathrm{d}\tau_{\mathrm{disp}}}{\mathrm{d}\lambda}\right)\left(\frac{1}{\lambda} - \frac{1}{\lambda_0}\right) - \tau_{\mathrm{GVD}}\right) \times \mathrm{e}^{-2\left(\lambda_0^2\left(\frac{\mathrm{d}\tau_{\mathrm{disp}}}{\mathrm{d}\lambda}\right)\left(\frac{1}{\lambda}-\frac{1}{\lambda_0}\right)-\tau_{\mathrm{GVD}}\right)^2 \Big/ \tau^2}$$

$\mathrm{d}\tau_{\mathrm{disp}}/\mathrm{d}\lambda$ denotes probe's chirp in wavelength domain.

The model discussed was experimentally verified using two independently set-up transient absorption spectrometers.

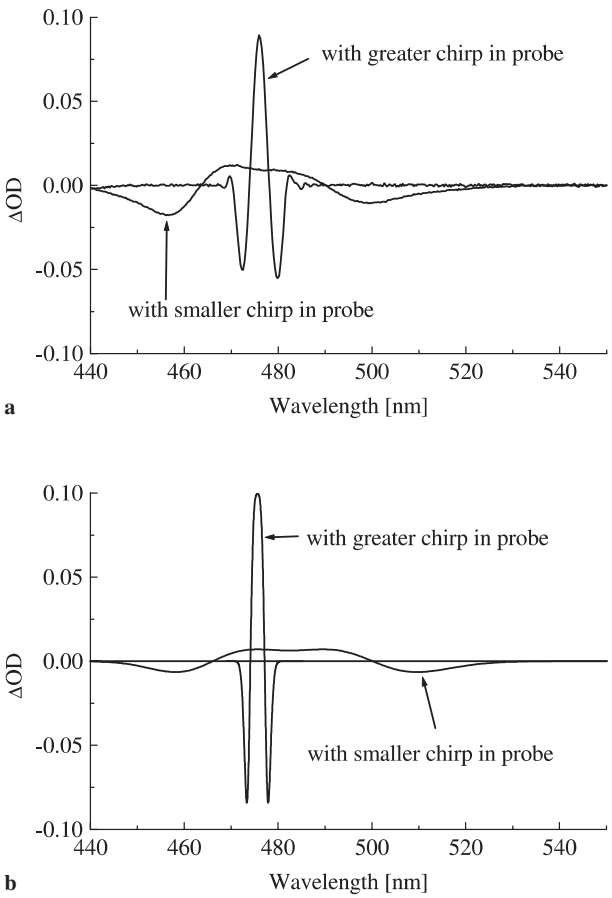

FIGURE 6 The influence of temporal chirp induced by dispersion along probe's path on XPM signal. Experimental data: XPM signal measured in 2.5-mm-thick sample with MeOH (**a**) and corresponding simulation, see (14), (**b**). Smaller chirp, after adding 6 mm of quartz to probe's optical path; larger chirp, 100 mm of MeOH

Figure 5 depicts a selection of measured XPM signals together with corresponding theoretical curves, calculated using (14).

A common feature of these signals is their broadening and decreasing amplitude with increased wavelength due to sample-imposed GVD. With sufficient spectral separation between the pump and the probe, the signal's maximum is split in two. In addition, it can be seen that the plots of the elaborated analytical formulae are spectrally narrower than those actually measured. This slight discrepancy is believed to originate from the white light continuum allegedly being composed of instantaneous frequency modes. However, if each mode within the probe pulse has a finite duration, then a greater number of modes interact simultaneously with the pump pulse, thus the broader spectral range undergoes modifications.

Figure 6 shows the importance of the white light continuum's temporal chirp on the XPM intensity. The smaller the chirp the smaller the signal's amplitude and the more it spreads spectrally.

Since the frequency is related to time through the chirp (9a,b), the XPM signals in time and wavelength domains look alike.

It should be noted that the analysis of XPM developed includes numerous approximations; therefore its validity is of a qualitative rather than quantitative nature. However, very simple formalism, practically limited to (8), describing the complicated temporal evolution of the XPM should be seen as an advantage. So far the discussions of the XPM effect in pump–probe measurements have been rather scarce. Rigorous mathematical treatment of the phenomena by other authors [7, 19] resulted in quite complex formulas, nonetheless strict, which still disregarded the GVD effect in the sample. The inclusion of GVD [20] to the considerations forced a numerical treatment, for which physical interpretation of some parameters can be ambiguous. In particular, how the probe's temporal chirp affects the XPM signal has not been studied so far. Compensation of the chirp can dramatically reduce this artifact. Moreover, because second term in the sum of (13) is usually much less than 1, the logarithm can be expanded and reads

$$S(t) \approx 0.86 \frac{\alpha\omega_0}{\beta\tau^2\tau_{\mathrm{GVD}}} \left(t\,\mathrm{e}^{-2t^2/\tau^2} - (t-\tau_{\mathrm{GVD}})\,\mathrm{e}^{-2(t-\tau_{\mathrm{GVD}})^2/\tau^2} \right) \tag{15}$$

so that $S(t)$ is directly proportional to the pump pulse intensity (A_0^2 proportional to α, (12)). Experimental confirmation of this expression is shown in Fig. 3b.

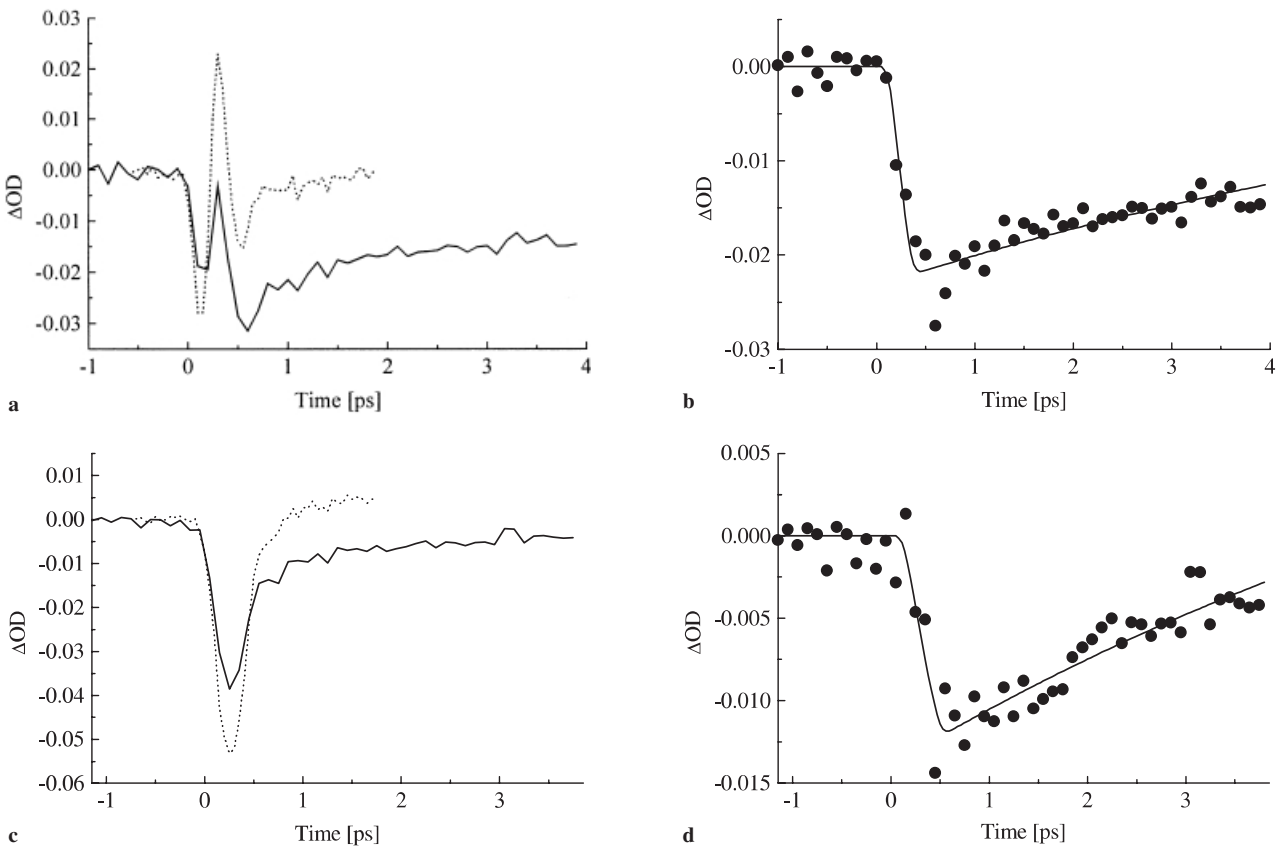

FIGURE 7 Result of applying the procedure of subtracting unwanted signals from measured transient absorption spectra of xanthione molecules (XT) in benzene solution (concentration of 10^4 M): **a** the kinetic of transient absorption taken at 420 nm for pure benzene with pump pulse energy of 52 μJ (*dotted*) and for XT in benzene solution with pump pulse energy of 38 μJ (*solid*); **b** experimental points at 420 nm after subtracting unwanted signals as in the procedure (*circles*) and fitted convolution of the response function with one-exponential decay of time constant equal 8.0 ± 0.4 ps (*solid*); **c** the kinetic of transient absorption taken at 447 nm for pure benzene with pump pulse energy of 52 μJ (*dotted*) and for XT in benzene solution with pump pulse energy of 38 μJ (*solid*); **d** experimental points at 447 nm after subtracting unwanted signals as in the procedure (*circles*) and fitted convolution of the response function with one-exponential decay of time constant equal 8.7 ± 0.8 ps (*solid*)

4 Procedure for artifacts subtraction

All unwanted signals, generated in pure solvents, were shown to have a linear dependence on the pump pulse intensity. This allows the writing of a very simple recipe for calculating an artifacts-free signal, S_c, originating from systems studied

$$S_c = S - S_r \frac{E_s}{E_r} f \ , \tag{16}$$

where S denotes uncorrected signal measured for excitation energy E_s and S_r is the signal pertaining to the solvent measured for pump pulse energy E_r. The factor f describes a decrease of mean energy in the sample due to stationary absorption (OD) by the molecules investigated

$$f = \frac{1}{L} \int_0^L 10^{-OD\frac{x}{L}} \, \mathrm{d}x = \frac{1 - 10^{-OD}}{2.3OD} \ . \tag{17}$$

For instance, when $OD = 0.15$ then $f = 0.85$, when $OD = 0.3$ then $f = 0.72$ and when $OD = 1$ then $f = 0.39$.

This correction procedure was applied for studies of xanthione (XT) molecules in benzene solution (Fig. 7). This figure shows the kinetics of S_2-XT observed in two spectral bands – that of 420 nm lying in the ground state depletion band and that of 447 nm lying in the stimulated S_2-fluorescence band. The first kinetic is obfuscated by XPM, which manifests itself by imposing an oscillatory feature onto the measured signal (Fig. 7a). The second kinetic is strongly affected by SRA (Fig. 7c), which is manifested by a dip, or a peak (see Sect. 3.2). Application of the procedure developed permitted determination of single-exponential decay time of the S_2-XT state, which was 8 ps. This value was later confirmed using a time-correlated single-photon counting technique [21]. The plot of fitted convolution of the single exponent with the pump–probe cross-correlation function (6) to the artifacts-free S_2 state decay is shown in Fig. 7b and d.

A major experimental problem, intrinsic to this type of measurements, is the sensitivity of the signal to spatial overlap between pump and probe. It is essential that both experiments, in pure solvent and in solution, be done keeping perfectly identical geometry, which turns out to be particularly difficult.

5 Conclusions

We have shown that unwanted signals generated during transient absorption measurements with fs resolution can notably distort weak transient spectra and in consequence render data analysis ambiguous. Reducing the contribution of unwanted signals to measured transient spectra can be done in the following ways:

- using white light continuum with small temporal chirp;
- using solvents with low third order non-linear susceptibility, $\chi^{(3)}$;
- preparing solutes with high absorbances, if sufficiently soluble, unless dimmer formation is a likely consequence;
- using cells with thin windows, preferably of low dispersion material (calcium fluoride);
- keeping an optically and spatially uniform layer in the liquid jet.

If the above conditions cannot be fulfilled it is necessary to make additional measurements in pure solvent and then carry out an elaborate post-experimental correction procedure.

ACKNOWLEDGEMENTS This work was partially supported by the National Committee for Scientific Research (KBN), Grant Nos. 3 TO9A 150 19 and 2 P03B 136 19. The experiments were performed at the Center for Ultrafast Laser Spectroscopy at the University of A. Mickiewicz in Poznan and in the Femtosecond Laboratory of Dr.G. Buntinx (LASIR) in Lille.

Appendix

Here we give an analytical treatment of the XPM. To each mode of a given frequency belong a number of photons, the square of which should be proportional to the probe's intensity at this frequency. The density of modes can be expressed as the inverse of the slope from Fig. 4a, unless the modulation is so strong that the slope changes sign. The expression then reads

$$I_{\mathrm{ref}}(\lambda) \propto \left(\left(\frac{\mathrm{d}\omega_{\mathrm{ref}}}{\mathrm{d}t} \right)^{-1} \right)^2 \tag{A.1}$$

$$I_{\mathrm{probe}}(\lambda) \propto \left(\left(\frac{\mathrm{d}\omega_{\mathrm{probe}}}{\mathrm{d}t} \right)^{-1} \right)^2 \ . \tag{A.2}$$

By introducing this expression into (1) and taking into account (9a), the resulting signal S is now given by

$$S = 2 \log \left(\frac{1}{\beta} \frac{\mathrm{d}\omega_{\mathrm{probe}}}{\mathrm{d}t} \right) \ . \tag{A.3}$$

If pump and probe wavelengths are different, the GVD effect has to be taken into account [12]. In brief, each sample layer contributes a specific signal for different pump–probe delays. Assuming a small enough frequency modification due to XPM (third term in (11) is much smaller than the second one)

$$\omega_{\mathrm{probe}}(t) = \omega_0 + \beta t + \frac{\alpha\omega_0}{\tau^2} \frac{1}{L} \times \int_0^L \left(t - \tau_{\mathrm{GVD}} \frac{x}{L} \right) \mathrm{e}^{-2(t - \tau_{\mathrm{GVD}} \frac{x}{L})^2/\tau^2} \, \mathrm{d}x \ , \tag{A.4}$$

where τ_{GVD} is the difference between the transit time of the pump and the probe through the sample cell of thickness L (compare (6)). Integrating in the sample length limits and taking time derivative of (A.4) leads to the following formula

$$\frac{\mathrm{d}\omega_{\mathrm{probe}}}{\mathrm{d}t} = \beta + \frac{\alpha\omega_0}{\tau^2 \tau_{\mathrm{GVD}}} \times \left(t \, \mathrm{e}^{-2t^2/\tau^2} - (t - \tau_{\mathrm{GVD}}) \, \mathrm{e}^{-2(t - \tau_{\mathrm{GVD}})^2/\tau^2} \right) \ . \tag{A.5}$$

Introducing (A.5) into (A.3) leads to (13).

REFERENCES

1 J.C. Diels, W. Rudolph: *Ultrashort Laser Pulse Phenomena. Fundamentals, Techniques, and Applications on a Femtosecond Time Scale* (Academic Press, London 1996)
2 C. Rulliere: *Femtosecond Laser Pulses* (Springer, Berlin, Heidelberg 1998)
3 Femtosecond Chemistry, ed. by J. Mainz, L. Wöste (VCH, New York 1995)
4 R. Naskrecki, M. Lorenc, M. Ziolek, J. Karolczak, J. Kubicki, A. Maciejewski, M. Szymanski: Bull. Pol. Acad. Sci. Chem. **47**, 333 (1999)
5 A. Maciejewski, R. Naskrecki, M. Lorenc, M. Ziolek, J. Karolczak, J. Kubicki, M. Matysiak, M. Szymanski: J. Mol. Struct. **555**, 1 (2000)
6 S. Pommeret, R. Naskrecki, P. van der Meulen, M. Menard, G. Vigneron, T. Gustavsson: Chem. Phys. Lett. **288**, 833 (1998)
7 S.A. Kovalenko, A.L. Dobryakov, J. Ruthmann, N.P. Ernsting: Phys. Rev. A **59**, 2369 (1999)
8 A. Reuther, A. Laubereau, D.N. Nikogosyan: Opt. Commun. **141**, 180 (1997)
9 R. Naskręcki, M. Meynard, P. Van der Meulen, G. Vigneron, S. Pommeret: Opt. Commun. **153**, 32 (1998)
10 M. Rasmusson, A.N. Tarnowsky, E. Åkesson, V. Sundström: Chem. Phys. Lett. **335**, 201 (2001)
11 *The Supercontinuum Laser Source*, ed. by R.R. Alfano (Springer, Berlin, Heidelberg 1989)
12 M. Ziolek, M. Lorenc, R. Naskrecki: Appl. Phys. B **72**, 843 (2001)
13 H. Kawano, T. Mori, Y. Hirakawa, T. Imsaka: Opt. Commun. **160**, 277 (1999)
14 T. Mori, Y. Hirakawa, T. Imasaka: Opt. Commun. **148**, 110 (1998)
15 W. Zinth, W. Kaiser: Opt. Commun. **32**, 507 (1980)
16 A. Mandl, R. Holmes, A. Flusberg, S. Fulgham, D. Angeley: J. Appl. Phys. **66**, 4625 (1989)
17 C.J. Hooker, J.M.D. Lister, P.A. Rodgers: Opt. Commun. **82**, 497 (1991)
18 P.L. Baldeck, R.R. Alfano: Phys. Rev. A **40**, 5063 (1989)
19 J.K. Wang, T.L. Chiu, C.H. Chiu, C.K. Sun: J. Opt. Soc. Am. B **16**, 651 (1999)
20 K. Ekvall, P. van der Meulen, C. Dhollande, L.E. Berg, S. Pommeret, R. Naskrecki, T. Gustavsson, J.C. Mialocq: J. Appl. Phys. **87**, 2340 (2000)
21 J. Karolczak, D. Komar, J. Kubicki, T. Wróżowa, K. Dobek, B. Ciesielska, A. Maciejewski: Chem. Phys. Lett. **344**, 154 (2001)